Original Article

Theoretical Evaluation of Furanone and its Derivatives for the Treatment of Cancer Through Eag-1 Inhibition

Abstract

Several studies suggest that some drugs such as astemizole and tetrandine can inhibit the expression of Eag-1 in cancer cells. Analyzing these data, this study aimed to evaluate the theoretical interaction of furanone (compound 1) and its derivatives (compounds 2 to 30) with Eag-1 using the 7CN1 protein as a theoretical model; in addition, astemizole, tetrandine, N-(4-(2-(Diethylamino)ethoxy)phenyl)-2-nitro-4-(trifluoromethyl)-aniline (DNTA), 1-Dimethylamino-3-[4-(2-nitro-4-trifluoromethyl-phenyl-amino)-phenoxy]-propan-2-ol (ZVS-08), and 3-Chloro-N-{2-[3,5-dibromo-4-(3-di-methyl-amino-propoxy)-phenyl]-ethyl}-4-metho-xy-benzamide (PD) were used as controls in the DockingServer software. Results showed that interaction of compounds 1-30, DNTA, ZVS-08, and PD with 7CN1 protein surface involves different aminoacid residues. Besides, inhibition constant was lower for furanone derivatives 7, 12, 16, 20, 25, 26, 29, and 30 compared to astemizole, tetrandine, DNTA, ZVS-08, and PD. These data suggest that furanone derivatives 7, 12, 16, 20, 25, 26, 29, and 30 could act as Eag-1 inhibitors in cancer cells. Therefore, these furenone derivatives could be good candidates for the treatment of cancer.

Keywords: *Cancer, Furanone, Eag-1, Docking*

Magdalena Alvarez-Ramirez[1], Lauro Figueroa-Valverde[2*], FranciscoDiaz-Cedillo[3], Marcela Rosas-Nexticapa[1], Maria Lopez-Ramos[2], Virginia Mateu-Armand[1], Lopez-Gutierrez Tomas[2]

[1]Nutrition Laboratory, Faculty of Nutrition, University of Veracruz, Medicos y s/n Odontologos 910210, Unidad del Bosque, Xalapa, Mexico.
[2]Pharmacochemistry Research Laboratory, Faculty of Biological-Chemical Sciences, University Autonomous of Campeche; Humberto Lanz Cárdenas s/n, Ex Hacienda Kalá, C.P. 24085, Campeche, Mexico. [3]Laboratory of Organic chemistry, Biological Sciences, National Politechnic Institute; Prolongacion de Carpio y Plan de Ayala s/n, Col. Sto Tomas, 11340, Mexico.

Address for correspondence:
Lauro Figueroa-Valverde, Departament of Chemistry, Laboratory of Pharmacochemistry Research, Faculty of Biological-Chemical Sciences, University Autonomous of Campeche; Humberto Lanz Cárdenas s/n, Ex Hacienda, 24085, Campeche Mexico.
E-mail: lfiguero@uacam.mx

Introduction

Cancer is one of the main public health problems worldwide;[1-4] this clinical pathology can be conditioned by several factors such as alcohol,[5, 6] obesity,[7, 8] cigarette smoking,[9, 10] dietary fatty acid pattern[11, 12] and some genetic factors.[13-15] In addition, other data indicates that the Eag-1 (ether-à-go-go-1; member of the voltage-dependent potassium channel family) may be involved in cancer cell growth.[16, 17] For example, a study showed the expression of Eag-1 potassium channels in gastric cancer patients using immunohistochemistry methods.[18, 19] Another study shows that both Eag-1 mRNA and protein expression is increased in A549 lung cancer cells undergoing epithelial-to-mesenchymal transition (a likely mechanism by which tumor cells become malignant) induced by TGFβ1 (growth factor beta).[20, 21] Besides, a report displayed that Eag-1 might be involved in the pathophysiological processes of prostate cancer tissue using both reverse transcription polymerase chain reaction (RT-PCR) and immunohistochemistry (IM) methods.[22, 23] Other studies carried out in a population of 12 Chinese women with breast cancer showed that this clinical pathology was associated with Eag-1 and HIF-1α expression.[24] In addition, Eag-1 expression was determined in esophageal squamous cell carcinomas tissues through both RT-PCR and IM methods.[25, 26] To try to inhibit the cancer cells' growth some drugs such as astemizole have been used; for example, a study suggests that astemizole may decrease cervical cancer cell lines growth (HeLa, SiHa, CaSki, INBL, and C-33A) by decreasing Eag1 expression.[27-29] Other data suggest that imipramine may produce changes in Eag1 expression on a prostate cancer cell line (DU145).[30, 31] Furthermore, a study showed that calcitriol can inhibit Eag1 expression and the proliferation of human breast cancer.[32, 33] All these data suggest that some drugs can inhibit the Eag1 expression translated as a decrease in cancer cell growth; however, the interaction of these drugs with Eag1 is not very clear on cancer cells. Analyzing these data, this study aimed to evaluate the possibility that a series of furanone derivatives could interact with Eag1 using a 7CN1 protein as a theoretical model. Besides, astemizole, tetrandine, DNTA, ZVS-08, and PD drugs were used as controls on the DockingServer program.

How to cite this article: Alvarez-Ramirez M, Figueroa-Valverde L, Diaz-Cedillo F, Rosas-Nexticapa M, Lopez-Ramos M, Mateu-Armand V, *et al*. Theoretical Evaluation of Furanone and its Derivatives for the Treatment of Cancer Through Eag-1 Inhibition. Clin Cancer Investig J. 2023;12(4):4-9. https://doi.org/10.51847/iVIQzRP5Lt

This is an open access journal, and articles are distributed under the terms of the Creative Commons Attribution-NonCommercial-ShareAlike 4.0 License, which allows others to remix, tweak, and build upon the work non-commercially, as long as appropriate credit is given and the new creations are licensed under the identical terms.

For reprints contact: Support_reprints@ccij-online.org

Access this article online

Website: www.ccij-online.org

DOI: 10.51847/iVIQzRP5Lt

Quick Response Code:

Materials and Methods

Methodology general

Figure 1 shows the chemical structure of furanone and its derivatives which were used as theoretical tools to assess their potential interaction with 7CN1.

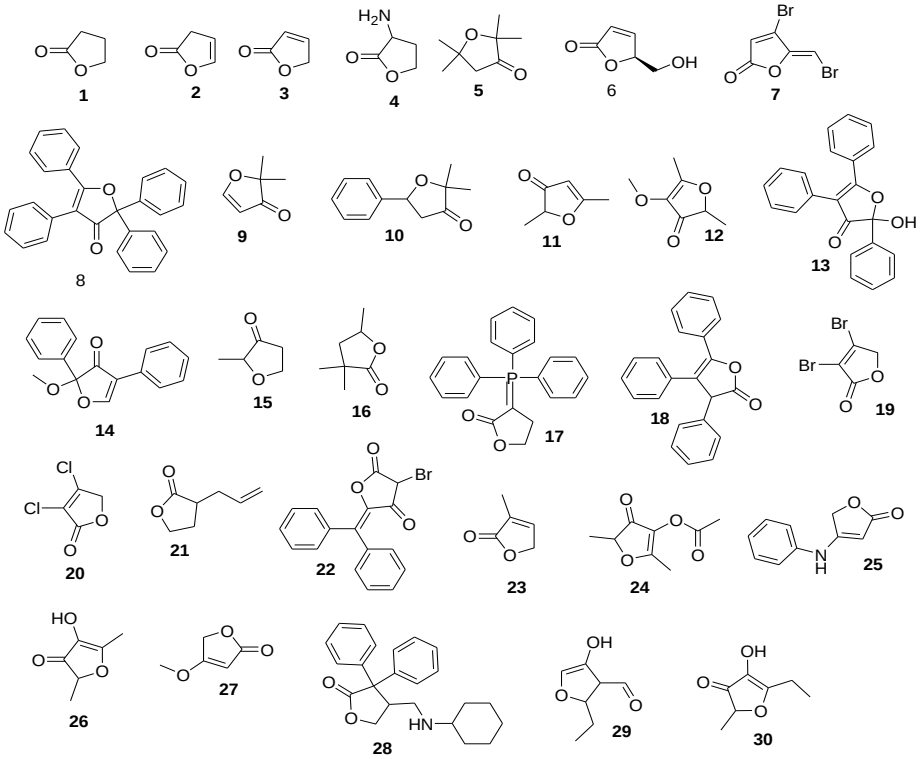

Figure 1. Chemical structure of furenone (1) and their derivatives (2-31). Source: ChemPub (https://pubchem.ncbi.nlm.nih.gov/).

1 = Dihydro-furan-2-one
2 = 3H-Furan-2-one
3 =5H-Furan-2-one
4 = Dihydro-3-amino-2-(3H)-furanone
5 = Dihydro-2,2,5,5-tetramethyl-3(2H)-furanone
6 = (S)-(-)-5-Hydroxymethyl-2(5H)-furanone
7 = (Z-)-4-Bromo-5-(bromomethylene)-2(5H)-fura-none
8 = 2,2,4,5-tetraphenyl-3(2H)-furanone
9 = 2,2-Dimethyl-3(2H)-furanone
10 = 2,2-Dimethyl-5-phenyl-dihydro-furan-3-one
11 = 2,5-Dimethyl-3(2H)-furanone
12 = 2,5-Dimethyl-4-methoxy-3(2H)-furanone
13 = 2-Hydroxy-2,4,5-triphenyl-3(2H)-furanone
14 = 2-Methoxy-2,4-diphenyl-3(2H)-furanone
15 = 2-Methyltetrahydro-3-furanone
16 = 3,3,5-trimethyldihydro-2(3H)-furanone
17 = 3-(Triphenylphosphoranylidene)dihydro-2(3H)-furanone
18 = 3,4,5-Triphenyl-2(3H)-furanone
19 = 3,4-Dibromo-2(5H)-furanone
20 = 3,4-Dichloro-2(5H)-furanone
21 = 3-Allyldihydro-2(3H)-furanone
22 = 3-Bromo-5-(Diphenylmethylene)-2(5H)-furo-none
23 = 3-Methyl-2(5H)-furanone
24 = 4-Acetoxy-2,5-dimethyl-3(2H)furanone
25 = 4-Anilino-2(5H)-furanone
26 = 4-Hydroxy-2,5-dimethyl-3(2H)-furanone
27 = 4-Methoxy-2(5H)-furanone
28 = 4-[(Cyclohexylamino)methyl]-3,3-diphenyl-dihydro-2(3H)-furanone
29 = 5-Ethyl-3-hydroxy-4-methyl-2(5H)-furenone
30 = 5-Ethyl-4-hydroxy-2-methyl-3(2H)-furanone

Ligand-protein complex

The interaction of furanone and their derivatives with the Eag1 protein surface was determined using 7CN1 (PDB DOI: https://doi.org/10.2210/pdb7CN1/pdb) protein[34] as a theoretical model. In addition, to evaluate the thermodynamic parameters involved in coumarin derivative-protein complex formation, the DockingServer program was used.[35]

Pharmacokinetics parameter

Theoretical pharmacokinetics involved in the chemical structure of furanone derivatives (7, 12, 16, 20, 25, 26, 29, and 30) were determined using the SwissADME software.[36]

Toxicity analysis

Toxicity evaluation for furanone derivatives 7, 12, 16, 20, 25, 26, 29, and 30 was determined using GUSAR software.[37]

Results and Discussion

Protein-ligand evaluation

In the literature, there are some methods to predict the interaction of some drugs with EAG-1 such as Autodock[38] and Rosetta[39]. In this way, a study showed that tetrandrine directly interacted with Eag1 through the amino acids Ile_{550}, Thr_{552}, and Gln_{557} surface[40]. Another study showed that procyanidin B1 could interact with the EAG-1 surface which involves amino acid residues such as Ile_{550}, Thr_{552}, and Gln_{557}. Analyzing these data, in this research furanone and its derivatives were used to evaluate their interaction with EAG-1 using 7CN1 protein as a theoretical model. The results shown in **Table 1** indicate that the interaction of furanone and their derivatives with the 7CN1 protein surface could involve some different aminoacid-residues compared to astemizole, tetrandine, DNTA, ZVS-08, and PD drugs.

Table 1. Aminoacid residues involved in the coupling of furenone and their derivatives with 7CN1 protein surface using DockingServer

Compounds	Aminoacid residues
Astemizole	Pro_{426}, Leu_{529}, Leu_{532}, Val_{533}, Thr_{556}, Leu_{559}, Trp_{563}, Cys_{566}, Ile_{567}
Tetrandine	Leu_{529}, Leu_{532}, Val_{533}, Ile_{560}, Trp_{563}, Ile_{567}
DNTA	Leu_{529}, Leu_{532}, Val_{533}, Val_{535}, leu_{552}, Thr_{556}, Trp_{563}
ZVS-08	Pro_{426}, Leu_{529}, Leu_{532}, Val_{533}, Ala_{536}, Trp_{563}, Ile_{567}
PD	Leu_{532}, Ile_{560}, Trp_{563}, Leu_{564}, Ile_{567}, Ile_{647}
1	Asp_{411}, Ile_{414}, Leu_{415}, Val_{418}, Phe_{463}, Arg_{534}, Val_{535}, Lys_{538}, Tyr_{542}
2	Asp_{411}, Ile_{414}, Leu_{415}, Val_{418}, Phe_{463}, Arg_{534}, Val_{535}, Lys_{538}, Tyr_{542}
3	Asp_{411}, Ile_{414}, Leu_{415}, Val_{418}, Phe_{463}, Arg_{534}, Val_{535}, Lys_{538}, Tyr_{542}
4	Ile_{419}, , Leu_{552}, Cys_{555}, Thr_{556}, Leu_{559}
5	Val_{418}, Ile_{419}, Ala_{422}, Leu_{532}, Val_{535}, Leu_{559}
6	Leu_{415}, Val_{418}, Ile_{419}, Ala_{422}, Leu_{532}, Val_{535}, Leu_{552}, Leu_{559}
7	Leu_{415}, Val_{418}, Ile_{419}, Leu_{532}, Val_{535}, Tyr_{542} Leu_{552}, Cys_{555}, Thr_{556}, Leu_{559}
8	Ile_{419}, Ala_{422}, Leu_{532}, Val_{535}, Ala_{536}, Leu_{552}, Cys_{555}, Thr_{556}, Leu_{559}, Trp_{563}
9	Leu_{415}, Val_{418}, Ile_{419}, Val_{535}, Tyr_{542}, Leu_{552}
10	Thr_{425}, Pro_{426}, Ala_{429}, Thr_{526}, Leu_{529}, Trp_{563}, Cys_{566}, Ile_{567}
11	Val_{418}, Ile_{419}, Ala_{422}, Leu_{532}, Val_{535}, Leu_{552}, Leu_{559}
12	Leu_{415}, Val_{418}, Ile_{419}, Ala_{422}, Leu_{532}, Val_{535}, Leu_{552}, Leu_{559}
13	Ile_{419}, Leu_{532}, Val_{535}, Ala_{536}, Leu_{552}, Cys_{55}, Thr_{556}, Leu_{559}, Trp_{563}
14	Leu_{415}, Val_{418}, Ile_{419}, Val_{535}, Tyr_{542}, Leu_{552}, Leu_{553}, Thr_{556}, Leu_{559}
15	Leu_{415}, Val_{418}, Ile_{419}, Val_{535}, Tyr_{542}, Leu_{552}
16	Val_{418}, Ile_{419}, Ala_{422}, Leu_{532}, Val_{535}, Leu_{552}, Leu_{559}
17	Ile_{419}, Ala_{422}, Leu_{532}, Val_{535}, Ala_{536}, Leu_{552}, Thr_{556}, Leu_{559}, Trp_{563}
18	Leu_{415}, Val_{418}, Ile_{419}, Val_{535}, Leu_{539}, Leu_{552}, $Cys_{555}Thr_{556}$, Leu_{559}, Trp_{563}
19	Leu_{415}, Val_{418}, Ile_{419}, Leu_{532}, Val_{535}, Tyr_{542}, Leu_{552}, Leu_{559}
20	Val_{418}, Ile_{419}, Leu_{532}, Val_{535}, Leu_{552}, Leu_{559}
21	Leu_{415}, Val_{418}, Ile_{419}, Ala_{422}, Leu_{532}, Val_{535}, Tyr_{542}, Leu_{559}
22	Pro_{426}, Leu_{529}, Leu_{532}, Trp_{563}, Ile_{567}
23	Leu_{415}, Val_{418}, Ile_{419}, Val_{535}, Tyr_{542}, Leu_{552}
24	Val_{418}, Ile_{419}, Ala_{422}, Leu_{532}, Val_{535}, Leu_{552}, Cys_{555}, Thr_{556}, Leu_{559}
25	Val_{418}, Ile_{419}, Ala_{422}, Leu_{532}, Leu_{552}, Thr_{556}, Leu_{559}
26	Val_{418}, Ile_{419}, Leu_{532}, Leu_{552}, Leu_{559}
27	Leu_{415}, Val_{418}, Ile_{419}, Ala_{422}, Leu_{532}, Val_{535}, Tyr_{542}, Leu_{552}
28	Thr_{425}, Pro_{426}, Ala_{429}, Thr_{526}, Leu_{529}, Leu_{532}, Trp_{563}, Cys_{566}, Ile_{567}
29	Val_{418}, Ile_{419}, Ala_{422}, Leu_{532}, Leu_{552}, Leu_{559}
30	Leu_{415}, Val_{418}, Ile_{419}, Ala_{422}, Leu_{532}, Val_{535}, Leu_{552}, Leu_{559}

DNTA = N-(4-(2-(Diethylamino)ethoxy)phenyl)-2-nitro-4-(trifluoromethyl)-aniline; **ZVS-08** = 1-Dimethylamino-3-[4-(2-nitro-4-trifluoromethyl-phenyl amino)-phenoxy]-propan-2-ol; **PD** = 3-Chloro-N-{2-[3,5-dibromo-4-(3-di-methylamino-propoxy)-phenyl]-ethyl}-4-methoxy-benzamide.

However, it is important to mention that this interaction may involve some thermodynamic parameters such as the free energy of binding, electrostatic energy, total intermolecular energy, and 4) Van der Waals (vdW) + hydrogen bond (H-bond) + desolvation energy.[35] For this reason, in this study, some thermodynamic parameters involved in the interaction of furanone and its analogs with the 7CN1 protein surface were evaluated using the DockingServer program. The results **(Table 2)** display differences in bond-energy levels for furanone and their derivatives compared with astemizole, tetrandibne, DNTA, ZVS-08, and PD. Besides, the inhibition constant (Ki) was lower for furonone derivatives 7, 12, 16, 20, 25, 26, 29 and 30 compared to PD. Other results indicate that Ki for furanone derivatives 1-9, 11-13, 15, 16. 18-21, 23, and 25-30 were lower compared to astemizole. All these data suggest that these furanone derivatives **(Figure 2)** could act as EAG-1 inhibitors, resulting in a decrease in cancer cell growth.

Table 2. Thermodynamic parameters involved in the interaction of coumarin and their derivatives with 7CN1 protein surface using DockingServer software.

Compound	A	B	C	D	E	F
Aztemisole	-5.91	46.76	-8.29	0.38	-7.91	828.65
Tetrandine	-5.21.	151.33	-6.95	0.72	-6.22	769.28
DNTA	-4.65	389.22	-6.19	0.44	-5.75	728.23
ZVS-08	-5.41	108.97	-6.10	0.44	-5.66	638.51
Purperealidin analog	-3.57	2.42	-5.29	0.29	-4.99	674.35
1	-2.82	8.59	-3.00	0.18	2.82	220.51
2	-2.73	10.05	-2.47	-0.25	-2.73	217.38
3	-3.09	6.42	-2.75	-0.34	-3.09	217.50
4	-2.23	23.02	-2.93	0.39	-2.53	323.42
5	-4.15	910	-4.16	0.01	-4.15	418.33
6	-3.19	4.56	-2.88	-0.01	-2.89	321.75

7	-4.05	1.08	-4.04	0.00	-4.05	306.14
8	-6.48	17.81	-7.66	0.01	-7.64	734.20
9	-3.03	5.96	-3.03	0.00	-3.03	326.04
10	-5.16	164.40	-5.46	0.00	-5.46	473.79
11	-3.66	2.09	-3.20	-0.46	-3.66	333.45
12	-3.61	2.25	-3.46	-0.45	-3.91	418.17
13	-6.12	32.71	-7.01	0.00	-7.01	678.55
14	-5.56	83.62	-6.43	0.00	-6.44	612.84
15	-3.01	6.20	-3.01	0.00	-3.01	305.43
16	-3.81	1.60	-3.81	0.00	-3.81	354.91
17	-5.50	93.62	-6.89	0.01	-6.88	698.70
18	-6.47	18.23	-7.39	-0.01	-7.40	656.12
19	-3.21	4.45	-3.21	0.00	-3.21	277.67
20	-4.04	1.10	-4.04	0.00	-4.04	361.31
21	-3.42	3.10	-4.01	0.00	-4.00	365.16
22	-5.21	152.69	-5.84	-0.01	-5.85	512.90
23	-2.73	9.95	-2.74	-0.01	-2.73	303.10
24	-4.21	823.80	-4.31	-0.44	-4.75	453.04
25	-3.60	2.29	-4.20	0.00	-4.19	477.50
26	-3.66	2.07	-3.22	-0.44	-3.66	353.21
27	-2.56	13.24	-2.85	-0.01	-2.86	319.19
28	-7.14	5.83	-7.66	0.41	-7.25	605.97
29	-3.85	1.50	-3.70	-0.45	-4.15	403.21
30	-3.64	2.14	-3.49	-0.45	-3.94	387.40

A = Est: Free Energy of Binding (kcal/mol); **B** = Inhibition Constant, Ki (mM); **C** = vdW + Hbond + desolv Energy (kcal/mol); **D** = Electrostatic Energy (kcal/mol); **E** = Total Intermolec. Energy (kcal/mol); **F** = Interact. Surface; **DNTA** = N-(4-(2-(Diethylamino)-ethoxy)phenyl)-2-nitro-4-(trifluoromethyl)aniline; **ZVS-08** = 1-Dimethylamino-3-[4-(2-nitro-4-trifluoromethyl-pheny-lamino)-phenoxy]-propan-2-ol.

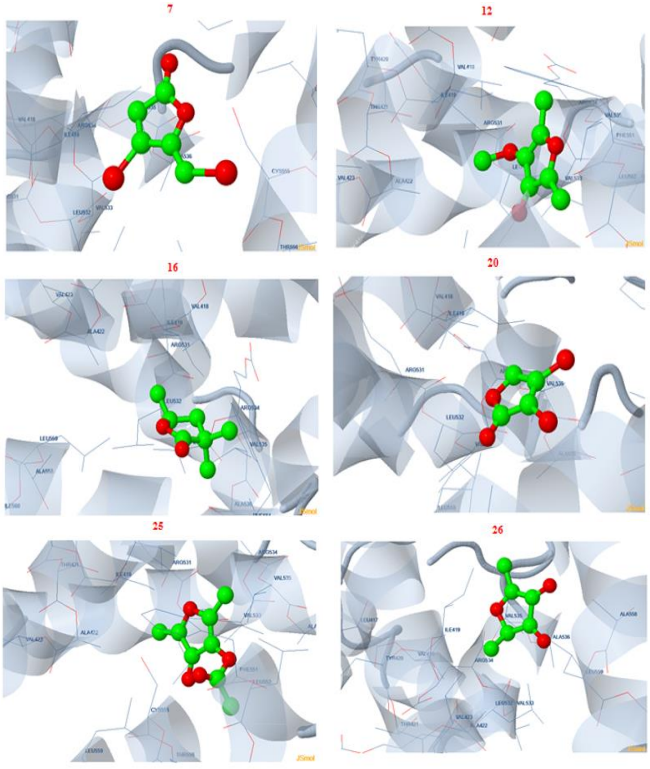

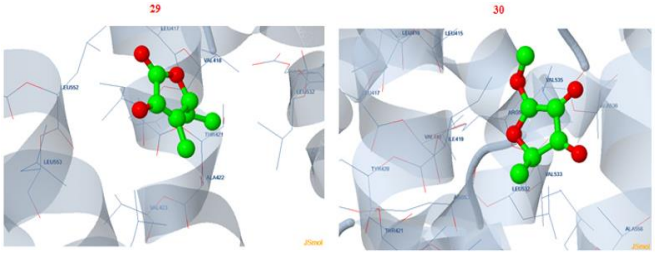

Figure 2. Interaction of furanone derivatives (7, 12, 16, 20, 25, 26, 29, AND 30) with 7CNC1 protein surface using Dockingserver software

Pharmacokinetic analysis

Different methods have been used to predict some pharmacokinetic parameters involved in some anticancer drugs.[41, 42] Analyzing these data, in this investigation, some pharmacokinetic parameters for furanone derivatives 7, 12, 16, 20, 25, 26, 29, and 30 were evaluated using the SwissADME program.[43] **Tables 3 and 4** showed the pharmacokinetic parameters involved in the possible gastrointestinal absorption and metabolism of furonone derivatives, which involve some cytochrome P450 systems. This phenomenon could depend on the chemical structure of furanone derivatives and their lipophilicity degree.

Table 3. Pharmacokinetic parameters for astemizole (i), tetrandine (ii), DNTA (iii), ZVS (iv), PD (v) and furanone derivative (7).

Parameter	*i*	*ii*	*iii*	*iv*	v	7
GI absorption	H	H	H	H	H	H
BBB permeant	Yes	No	No	No	Yes	Yes
P-gp substrate	Yes	No	No	Yes	No	No
CYP1A2 inhibitor	No	No	No	No	Yes	No
CYP2C19 inhibitor	Yes	No	Yes	Yes	Yes	No
CYP2C9 inhibitor	No	No	Yes	Yes	Yes	No
CYP2D6 inhibitor	Yes	No	Yes	Yes	Yes	Yes
CYP3A4 inhibitor	Yes	No	Yes	Yes	Yes	No
Consensus $LogP_{O/W}$	5.00	5.49	4.19	3.02	5.10	1.81

H = high; *i* = Astemizol; *ii* = tetrandine; *iii* DNTA; *iv* = ZVS-08; *v* = PD . GI = gastrointestinal; BBB = Blood-Brain-Barrier; P-gp = P-glycoprotein.

Table 4. Pharmacokinetic parameters for furanone derivatives 12, 16, 20, 25, 26, 29 and 30.

Parameter	12	16	20	25	26	29	30
GI absorpt	H	H	H	H	H	H	H
BBB perm	Yes	Yes	Yes	Yes	Yes	Yes	No
P-gp substrate	No	No	No	No	No	No	No
CYP1A2 inhibitor	No	No	No	Yes	No	No	No
CYP2C19 inhibitor	No	No	No	No	No	No	No
CYP2C9 inhibitor	No	No	No	No	No	No	No
CYP2D6 inhibitor	No	No	No	No	No	No	No
CYP3A4 inhibitor	No	No	No	No	No	No	No
Consensus $LogP_{O/W}$	0.92	1.63	1.41	1.47	0.56	0.56	0.25

Toxicity analysis

In the literature, there are some methods to predict the degree of toxicity of various compounds such as ADME/Tox,[44] eToxPred,[45] and GUSSAR.[46] This study aimed to evaluate the possible toxic effect produced by furanone derivatives 7, 12, 16, 20, 25, 26, 29, and 30 using the GUSSAR software.

The results shown in **Table 5** suggest that higher doses of furanone derivatives (7, 12, 16, 20,25, 26, and 29) are needed (via intraperitoneal) to produce toxicity compared to astemizol, tetrandine, DNTA, ZVS-08, AND PD drugs. Besides, other data indicate that furanone derivatives 7, 12, 16, 20,25, 26, 29, and 30 require higher doses (via oral) to induce toxicity compared to astemizol, tetrandine, DNTA, ZVS-08, AND PD drugs.

Table 5. Theoretical toxicity for furanone derivatives

Compound	IP LD50 (mg/kg)	IV LD50 (mg/kg)	Oral LD50 (mg/kg)	SC LD50 (mg/kg)
Astemizole	253.30	36.59	835.00	710.90
Tetrandine	70.92	65.40	708.30	121.80
DNTA	345.80	84.54	992.80	473.80
ZVS-08	286.40	83.93	727.30	579.20
PD	330.10	80.65	960.00	4990.00
7	496.40	29.71	910.00	856.40
12	263.20	40.96	872.00	651.50
16	426.00	14.56	2726.00	951.30
20	726.30	18.92	785.30	1242.00
25	653.70	32.21	909.50	1084.00
26	125.90	42.37	861.10	565.80
29	385.50	60.90	1975.00	727.70
30	181.40	67,78	1322.00	522.80

IP = Intraperitoneal.
IV = Intravenous.
Oral = Oral.
SC = Subcutaneous.

Conclusion

In this research, the theoretical interaction of furanone and its derivatives with Eag-1 was determined. The results showed a higher affinity of furanone derivatives 7, 12, 16, 20, 25, 26, 29, and 30 for Eag-1 surface compared to astemizol, tetrandine, DNTA, ZVS-08 AND PD drugs. All these data suggest that furanone derivatives 7, 12, 16, 20, 25, 26, 29, and 30 could act as Eag-1 inhibitors. This phenomenon could be translated as good candidates for the treatment of cancer cells.

Acknowledgments
None.

Conflict of interest
None.

Financial support
None.

Ethics statement
All procedures in this study were performed in accordance with protocols for Pharmacochemistry Laboratory of University Autonomous of Campeche.

References

1. Xia C, Dong X, Li H, Cao M, Sun D, He S, et al. Cancer statistics in China and United States, 2022: profiles, trends, and determinants. Chin Med J. 2022;135(5):584-90.
2. Siegel R, Miller K, Fuchs H, Jemal A. Cancer statistics, 2022. Cancer J Clin. 2022;72(1):7-33.
3. Saad M, Mokrab Y, Halabi N, Shan J, Razali R, Kunji K, et al. Genetic predisposition to cancer across people of different ancestries in Qatar: A population-based, cohort study. Lancet Oncol. 2022;23(3):341-52.
4. Lazarus E, Bays H. Cancer, and obesity: an obesity medicine association (OMA) clinical practice statement (CPS) 2022. Obes Pill. 2022;3:100026.
5. Yoo J, Han K, Shin D, Kim D, Kim B, Chun S. Association Between Changes in Alcohol Consumption and Cancer Risk. J Am Med Assoc. 2022;5(8):e2228544.
6. Im P, Yang L, Kartsonaki C, Chen Y, Guo Y, Du H. Alcohol metabolism genes and risks of site-specific cancers in Chinese adults: An 11-year prospective study. Int J Cancer. 2022;150(10):1627-39.
7. Lazarus E, Bays H. Cancer, and obesity: an obesity medicine association (OMA) clinical practice statement (CPS) 2022. Obes Pill. 2022;3:100026.
8. Aminian A, Wilson R, Al-Kurd A, Tu C, Milinovich A, Kroh M. Association of bariatric surgery with cancer risk and mortality in adults with obesity. J Am Med Asocc. 2022;327(24):2423-33.
9. Hecht S, Hatsukami D. Smokeless tobacco and cigarette smoking: chemical mechanisms and cancer prevention. Nat Rev Cancer. 2022;22(3):143-55.
10. Phua Z, MacInnis R, Jayasekara H. Cigarette smoking and risk of second primary cancer: a systematic review and meta-analysis. Cancer Epidemiol. 2022;78:102160.
11. Wan Y, Wu K, Wang L, Yin K, Song M. Dietary fat and fatty acids in relation to risk of colorectal cancer. Eur J Nut. 2022;61(4):1863-73.
12. Tu K, Ma T, Zhou R, Xu L, Fang Y, Zhang C. Association between Dietary Fatty Acid Patterns and Colorectal Cancer Risk: A Large-Scale Case-Control Study in China. Nutrients. 2022;14(20):4375.
13. Huang F, Yu S. Esophageal cancer: risk factors, genetic association, and treatment. Asian J Surg. 2018;41(3):210-5.
14. O'Sullivan D, Sutherland R, Town S, Chow K, Fan J, Forbes N, et al. Risk factors for early-onset colorectal cancer: a systematic review and meta-analysis. Clin Gastroent Hepatol. 2022;20(6):1229-40.
15. Lee A, Yang X, Tyrer J, Gentry-Maharaj A, Ryan A, Mavadda, N, et al. Comprehensive epithelial tubo-ovarian cancer risk prediction model incorporating genetic and epidemiological risk factors. J Med Genet. 2022;59(7):632-43.
16. Pardo L, Stühmer W. Eag1 as a cancer target. Exp Opin Ther Targets. 2008;12(7):837-43.
17. Rodríguez-Rasgado J, Acuña-Macías I, Camacho J. Eag1 channels as potential cancer biomarkers. Sensors. 2012;12(5):5986-95.
18. Ding X, Luo H, Jin X, Yan J, Ai Y. Aberrant expression of Eag1 potassium channels in gastric cancer patients and cell lines. Med Oncol. 2007;24:345-50.
19. Fawzy A, Alqelaiti YA, Almatrafi MM, Almatrafi OM, Alqelaiti EA. Common Sensitive Prognostic Markers in Breast Cancer and their Clinical Significance: A Review Article. Arch Pharm Pract. 2022;13(1):40-5.
20. Hemdan DII, Abdulmaguid NYM. A Comparative of Nutritional Impacts of Pomegranate and Beetroot on Female Mice Bearing Ehrlich Ascites Carcinoma. Arch Pharm Pract. 2021;12(3):48-54.
21. Sun Y, Chen Q, Liu P, Zhao Y, He Y, Zheng X, et al. Impact of Traditional Chinese Medicine Constitution on Breast Cancer Incidence: A Case-Control and Cross-Sectional Study. Pharmacophore. 2021;12(2):46-56.
22. Aloufi BH. Structure-based Multi-targeted Molecular Docking and Molecular Dynamic Simulation Analysis to Identify Potential Inhibitors against Ovarian Cancer. J Biochem Technol. 2022;13(2):29-39.
23. Abubaker SA, Abdelwadoud ME, Ali MM, Ahmad HA, Khlafalla AM, Elmahi OM, et al. Immunohistochemical Expression of Oestrogen and Epidermal Growth Factor Receptors in Endometrial Cancerous in Sudanese Patients. J Biochem Technol. 2021;12(1):58-62.
24. Aloufi BH, Alshammari AM. Graphical Data Representation and Analytics to Link the Potential Interaction for Lung Cancer Genes. Int J Pharm Res Allied Sci. 2022;11(2):62-72.

25. Awang ABC, Mutalip SSM, Mohamed R, Nordin M, Siew JSK, Dasiman R. A Review of the Effects of Vitamin E in Ovarian Cancer. Int J Pharm Res Allied Sci. 2022;11(2):81-5.
26. Sahebzadeh M, Khuzani HR, Keyvanara M, Tabesh E. Explaining the Factors Shaping Two Different Beliefs about Cancer in Iran Based on Causal Layer Analysis "CLA". Entomol Appl Sci Lett. 2021;8(2):42-50.
27. Restrepo-Angulo I, Sanchez-Torres C, Camacho J. Human EAG1 potassium channels in the epithelial-to-mesenchymal transition in lung cancer cells. Anticancer Res. 2011;31(4):1265-70.
28. Zheng Y, Li Z, Gao X, Zhang X, Li F, Shi Y, et al. Expression of Eag1 K (+) channel in prostate cancer and its significance. Zhonghua nan ke xue. Nat J Androl. 2013;19(3):205-9.
29. Lai Q, Wang T, Guo Q, Zhang Y, Wang Y, Yuan L, et al. Positive correlation between the expression of hEag1 and HIF-1α in breast cancers: an observational study. BMJ open. 2014;4(5):e005049.
30. Ding X, Wang X, Luo H, Tan S, Gao S, Luo B, et al. Expression and prognostic roles of Eag1 in resected esophageal squamous cell carcinomas. Dig Dis Sci. 2008;53:2039-44.
31. De-Guadalupe Chávez-López M, Hernández-Gallegos E, Vázquez-Sánchez A, Gariglio P, Camacho J. Antiproliferative and proapoptotic effects of astemizole on cervical cancer cells. Int J Gynecol Cancer. 2014;24(5):824-8.
32. Gubič Š, Toplak Ž, Shi X, Dernovšek J, Hendrickx L, Pinheiro-Junior E, et al. New Diarylamine KV10. 1 Inhibitors and Their Anticancer Potential. Pharmaceutics. 2022;14(9):1963.
33. Söğüt F, Çömelekoğlu Ü, Dervişoğlu H, Eroğlu P, Yalin S, Yilmaz N. Effect of imipramine on ether à-go-go potassium channel (Kv1. 10) expression in DU145 prostate cancer cells. Andrologia. 2022;54(1):e14291.
34. Data Bank Protein. Available from: https://www.rcsb.org/structure/7cn1
35. Figueroa-Valverde L, Rosas-Nexticapa M, Montserrat M, Díaz-Cedillo F, López-Ramos M, Alvarez-Ramirez M, et al. Synthesis and Theoretical Interaction of 3-(2-oxabicyclo [7.4. 0] trideca-1 (13), 9, 11-trien-7-yn-12-yloxy)-steroid Derivative with 17β-hydroxysteroid Dehydrogenase Enzyme Surface. Biointerface Res Appl Chem. 2023;13:266.
36. Figueroa-Valverde L, Rosas-Nexticapa M, Alvarez-Ramirez M, López-Ramos M, Díaz-Cedillo F, Mateu-Armad M. Evaluation of Biological Activity Exerted by Dibenzo [b, e] Thiophene-11 (6H)-One on Left Ventricular Pressure Using an Isolated Rat Heart Model. Drug Res. 2023:263-70.
37. Da-Rocha M, Marinho E, Marinho M, Dos Santos H. Virtual screening in pharmacokinetics, bioactivity, and toxicity of the amburana cearensis secondary metabolites. Biointerface Res Appl Chem. 2022;12:8471-91.
38. Xu X, Song Z, Yin Y, Zhong F, Song J, Huang J, et al. Virtual Screening of Inhibitors for Chitosanases EAG1. Adv Enz Res. 2020;8(4):49-57.
39. Emigh A, DeMarco K, Furutani K, Bekker S, Sack J, Clancy C, et al. Structural Modeling of hERG Channel Interactions with Drugs using Rosetta. Biophys J. 2018;114(3):486a.
40. Wang X, Chen Y, Li J, Guo S, Lin X, Zhang H, et al. Tetrandrine, a novel inhibitor of ether-à-go-go-1 (Eag1), targeted to cervical cancer development. J Cell Physiol. 2019;234(5):7161-73.
41. Levitt D. PKQuest: a general physiologically based pharmacokinetic model. Introduction and application to propranolol. BMC Clin Pharmacol. 2002;2(1):1-21.
42. Ishaku S, Bakare-Odunola M, Musa A, Yakasai I, Garba M, Adzu B. Effect of dihydro-artemisinin on the pharmacokinetics of gliclazide in diabetic subjects. Int J Biol Chem Sci. 2020;14(6):2267-76.
43. Sicak Y. Design and antiproliferative and antioxidant activities of furan-based thiosemicarbazides and 1, 2, 4-triazoles: their structure-activity relationship and SwissADME predictions. Med Chem Res. 2021;30(8):1557-68.
44. Li A. Screening for human ADME/Tox drug properties in drug discovery. Drug Dis Today. 2001;6(7):357-66.
45. Pu L, Naderi M, Liu T, Wu H, Mukhopadhyay S, Brylinski M. eToxPred: a machine learning-based approach to estimate the toxicity of drug candidates. BMC Pharmacol Toxicol. 2019;20(1):1-15.
46. Lagunin A, Zakharov A, Filimonov D, Poroikov V. QSAR modeling of rat acute toxicity on the basis of PASS prediction. Mol Inf. 2011;30(2-3):241-50.